Materials Science and Technology (MS&T) 2014
October 12-16, 2014, Pittsburgh, Pennsylvania, USA
Copyright © 2014 MS&T14®

Inhibition effect of Phenylamine on the Corrosion of Austenitic Stainless Steel (Type 304) in dilute sulphuric acid

R.T. Loto[1, 2]*, C. A. Loto[1, 2] and A.P.I. Popoola[2]

[1]Department of Mechanical Engineering, Covenant University, Ota, Ogun State, Nigeria

[2]Department of Chemical, Metallurgical & Materials Engineering, Tshwane University of Technology, Pretoria, South Africa

*tolu.loto@gmail.com

+2348084283392

Abstract. The corrosion of austenitic stainless steel (type 304) in dilute sulphuric acid solutions in addition to recrystalized sodium chloride concentrates in the presence of specific proportions of phenylamine was studied with the aid of polarization resistance technique, electrode potential monitoring and coupon method. Results showed the overwhelming influence of the compound in corrosion inhibition with an inhibition efficiency of 97.5% from coupon analysis and 86.10% from polarization test at highest observed concentration of the inhibitor. Corrosion potential measurement showed potentials well with passivation values. Corrosion rate decreased progressively with increase in concentration of phenylamine. Adsorption of the compound on the steel surface followed the Langmuir isotherm model. Thermodynamic calculations showed the interaction mode with the steel to be physiochemical. Observation from scanning electron microscopy and x-ray diffractometry showed the electrochemical impact on the surface topography and the phase compounds of the steel samples studied. Results from statistical analysis depict the sharp influence of inhibitor concentration on the electrochemical performance of the compound.

Keywords; Phenylamine; Sulphuric acid; Langmuir; Corrosion; Inhibition

Introduction

Millions of dollars are lost each year due to corrosion. Much of this is as a result of the corrosion of iron and steel. Corrosion damage causes leakage of fluids or gases in devices and containers made of alloy materials. Even more dangerous is the loss of strength of engineering structures induced by

Copyrighted content, licensed for the sole use of:
Roland Loto, (3454331)

corrosion leading to subsequent failure. Stainless steel (Type 304) is widely used in many applications such as desalination plants, construction materials, pharmaceutical industry, pickling process, oil and gas industry etc, due to their stability, good corrosion resistance, high strength, workability and weldability [1-5]. Stainless steels resist corrosion through the formation of a thin oxide layer enriched in chromium on the metal surface in acidic environments. In highly corrosive environments the protective passive surface layer of the steel is destroyed resulting in corrosion [6]. Corrosion has a strong influence in the oil industry, due to the location of production formations in hostile environments. Acids are consistently pumped into wells to enhance productivity [7-12].

Application of inhibitors is one of the most empirical methods for corrosion mitigation in corrosive media, often used to reduce the rate of dissolution of metals. [13-24]. Corrosion inhibitors are commonly added in small amounts to acid stimulation fluids, cooling waters, oil and gas production streams, either continuously or intermittently to control corrosion and during the pickling process. The inhibitors create a protective barrier against the corrosive species through adsorption which results in effective blocking of the active sites on the metal surface. Interests in corrosion inhibition have majorly been directed to organic compounds [25-27]. A significant number of researches have shown that organic compounds containing heteroatoms in their structure tends to be effective inhibitors. The study aims to investigate the corrosion inhibition efficiency and adsorption mechanism of phenylamine on austenitic stainless steel (type 304) in 3 M sulphuric solution.

Experimental procedure

Weight-loss experiments

Weighted test specimens were fully and separately immersed in 200 ml of the test media at specific concentrations of the phenylamine (AMB) for 360 h at ambient temperatures. Each of the test specimens was taken out every 72 h, washed with distilled water, rinsed with acetone, dried and re-weighed.

Open circuit potential measurement and Linear polarization resistance

A two-electrode electrochemical cell with a silver/silver chloride was used as reference electrode. OCP measurements were obtained with Autolab PGSTAT 30 ECO CHIMIE potentiostat. Resin mounted test specimens were immersed in the test solution at specific concentrations of AMB. The

Copyrighted content, licensed for the sole use of:
Roland Loto, (3454331)

potentiodynamic studies were then made from -1.5V *versus* OCP to +1.5 mV *versus* OCP at a scan rate of 0.00166 V/s and the corrosion currents were registered.

Scanning electron microscopy characterization and X-Ray diffraction analysis

The surface morphology of the uninhibited and inhibited steel samples was analysed after weight-loss test using Jeol scanning electron microscope for which SEM micrographs were recorded. X-ray diffractometry (XRD of the film formed without AMB addition was done using a Bruker AXS D2 phaser desktop powder diffractometer. Analysis of the steel sample inhibited with AMB was done with PANalytical X'Pert Pro powder diffractometer.

Statistical Analysis

Two-factor single level statistical analysis using ANOVA test (F - test) was performed so as to investigate the significant effect of inhibitor concentration and exposure time on the inhibition efficiency of AMB in the acid media.

Results and discussion

Weight-loss measurements

Decrease in corrosion rate is due to increase in concentration of AMB due to availability of more AMB molecules for adsorption on the alloy surface. This is responsible for increase in surface coverage of the alloy specimen as shown in Fig. 2, 3 & 4 which depicts the relationship between weight-loss, corrosion rate and percentage inhibition efficiency with exposure time at AMB concentrations while Fig. 5 shows the relationship between %*IE* and AMB concentration.

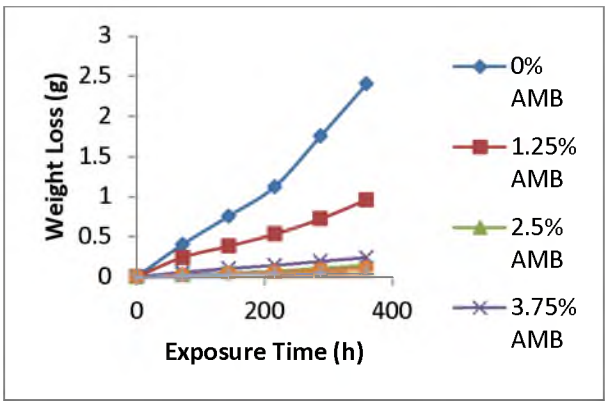

Figure 2: Variation of weight-loss with exposure time for samples (A – G) in 3 M H_2SO_4.

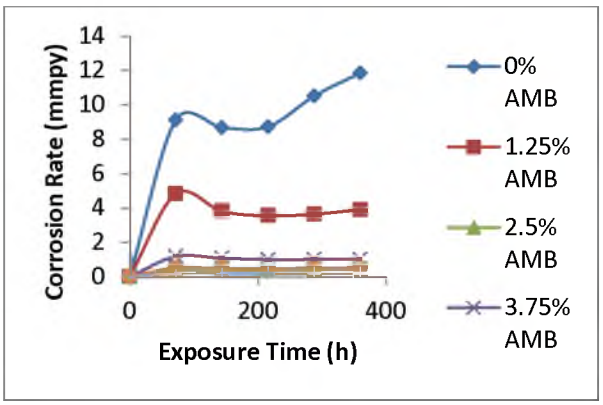

Figure 3: Effect of percentage concentration of AMB on the corrosion rate of austenitic stainless

Copyrighted content, licensed for the sole use of:
Roland Loto, (3454331)

steel in 3 M H_2SO_4

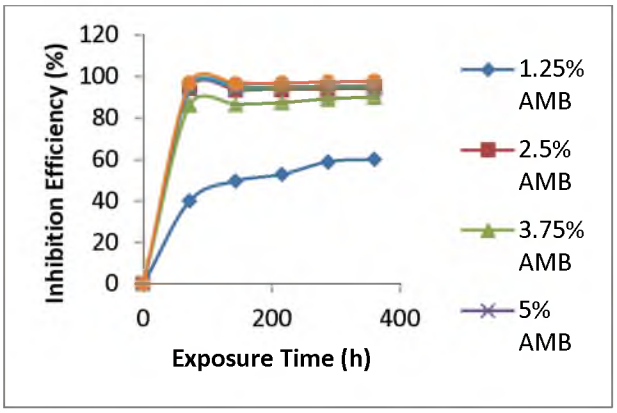

Figure 4: Plot of inhibition efficiencies of sample (A-G) in 3 M H_2SO_4 during the exposure period

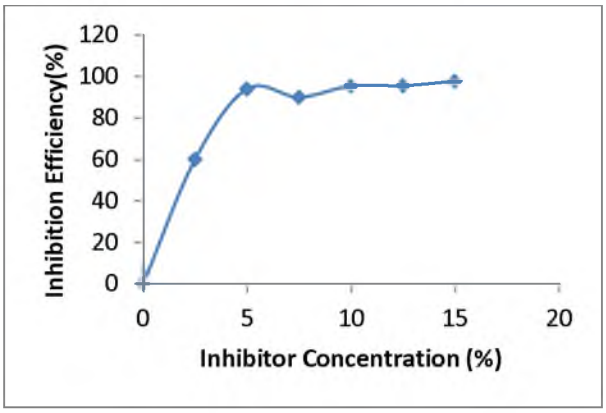

Figure 5: Variation of percentage inhibition efficiency of AMB with inhibitor concentration in 3 M H_2SO_4

Open Circuit Potential Measurement

The results from the open-circuit potential are shown in Fig. 6 respectively. In the test solutions a progressive potential displacement towards negative values was noticed in 0% AMB concentrations during the immersion hours. This corresponds with anodic dissolution of the steel specimen in the absence of AMB. At 1.25% AMB there is a gradual positive shift in corrosion potential to the noble direction due to the inhibitive action of AMB at this concentration. The influence of AMB on the electrochemical process is minimal as the corrosion potential after 288 h of exposure remains in the domain of intermediate corrosion. After 1.25% AMB, the increase in the number of AMB molecules at higher concentrations has a profound influence on the corrosion behaviour of the steel and the electrolytic action of the corrosion species. The average potential at 288 h after 1.25% AMB ranges between ~300 and 302 mV which is well within the zone of passivation potentials for stainless steel.

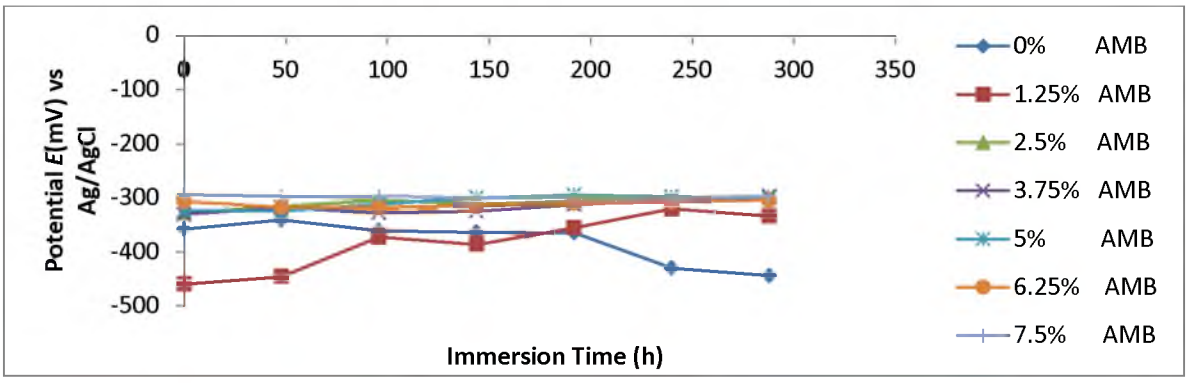

Copyrighted content, licensed for the sole use of:
Roland Loto, (3454331)

Figure 6: Variation of potential with immersion time for potential measurements in 3 M H_2SO_4

Polarization studies

The effect of the addition of AMB on the polarization curves of austenitic stainless steel type 304 in 3 M H_2SO_4 solutions at 25 °C was studied at ambient temperature as shown in Fig. 7. Results obtained using Tafel and linear polarization methods shows that AMB inhibited the electrochemical process of corrosion. The current density reduced sharply after 0% AMB concentration compared to all other AMB concentrations while the corrosion rate reduced drastically The adsorption of AMB is slightly independent of the value of its concentrations giving an average inhibition efficiency of 86% which was maintained after 1.25% AMB. The inhibitive action of the AMB is related to its adsorption and formation of a barrier film on the electrode surface.

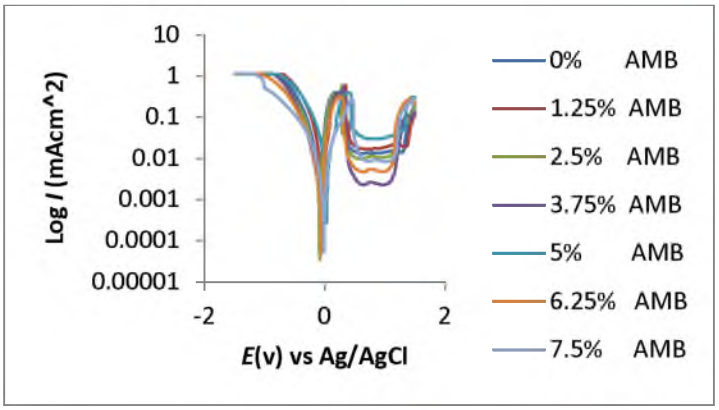

Figure 7: Plot of polarization scans at specific concentrations of AMB at 25 °C (0% - 7.5% AMB)

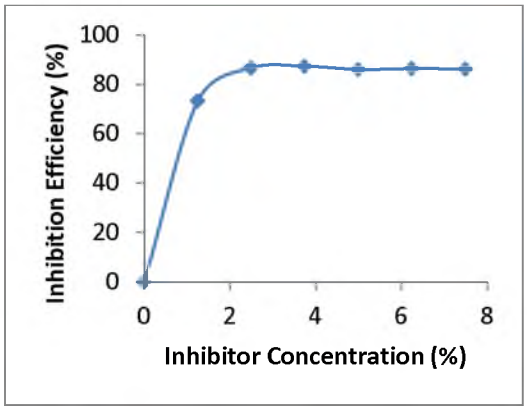

Figure 8: Relationship between %*IE* and inhibitor concentration for polarization test in 3 M H_2SO_4

AMB compound appeared to act as a mixed type inhibitor since both cathodic and anodic reactions were influenced by the presence of AMB in the corrosive medium. Corrosion potentials slightly shifted in both directions in H_2SO_4, while the maximum displacement in E_{corr} value is 65 mV, thus AMB is a mixed type inhibitor but with greater tendency for anodic inhibition [28, 29]. AMB adsorption is influenced by the electronic properties of its functional groups [30], i.e. the hydronium ion when it gains an electron and protonates in acid media. The results show that the mechanism of inhibition involves surface coverage of the steel sample by AMB molecules by physiochemical adsorption. AMB has an amino functional group (-NH_2), which protonates in the acid solution and

Copyrighted content, licensed for the sole use of:
Roland Loto, (3454331)

becomes a hydronium ion (NH^{+}_{3}). The ionized AMB molecule dominantly competes with the hydrogen atom for electrons thus inhibiting hydrogen evolution reactions.

Scanning electron Microscopy Analysis

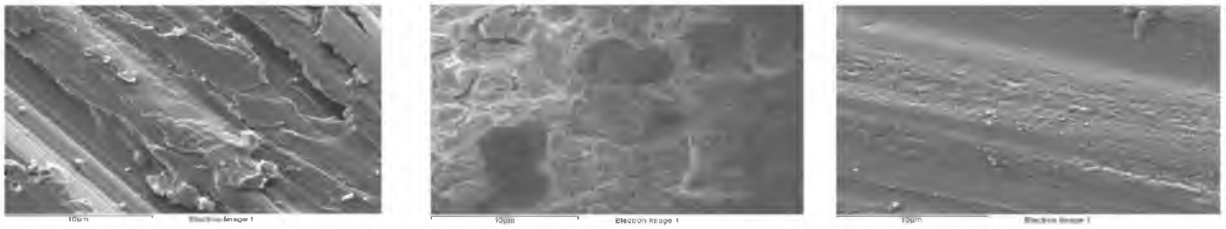

(a) (b) (c)

Figure9**:** SEM micrographs of: a) stainless steel, b) stainless steel in 3 M H_2SO_4, c) stainless steel in 3 M H_2SO_4 with AMB.

The micrograph (Fig. 9b) depict an irregular topography with micro hallows and perforations at high magnification. The micropits consist of sulphur and chloride atoms, thus proving the detrimental impact of these atoms on pit formation. They expedite the hydrolysis and electrolytic transport of charged iron atoms into the acid media after expulsing the preadsorbed oxygen ions. This phenomenon results in the rapid degradation and corrosion of the alloy specimen, leading to the formation and growth of voids on the passive film. The improved morphology of the steel sample (Fig. 9c) is due to the crystalline precipitation of AMB molecules in the acid solution on the steel surface compared with the uninhibited sample.

X-Ray Diffraction Analysis

X-ray diffraction (XRD) patterns of stainless steel surfaces from 3 M H_2SO_4 solutions are shown in Fig 10a & b respectively. The peak values at 2θ values for the steel in the solution without AMB (Fig.10) showed the presence of iron oxides due to the redox corrosion process that took place on the steel surface. The peaks at $2\theta = 89.4°$ and $111.2°$ for the uninhibited steel in 3 M H_2SO_4 (Fig. 10a) is attributed to iron (ii, iii) oxide (Fe_3O_4) while the peaks at $2\theta = 39.5°$ and $50.5°$ can be assigned to iron (iii) oxide (Fe_2O_3). Observation of the diffraction peaks for the inhibited steel (Fig. 10b) surfaces showed the absence of iron oxides and chemical compounds associated with corrosion. The compounds present especially chromium oxide at peak $2\theta = 51°$ is responsible for the passivation of the steel in addition to the effective inhibiting action of AMB.

Copyrighted content, licensed for the sole use of:
Roland Loto, (3454331)

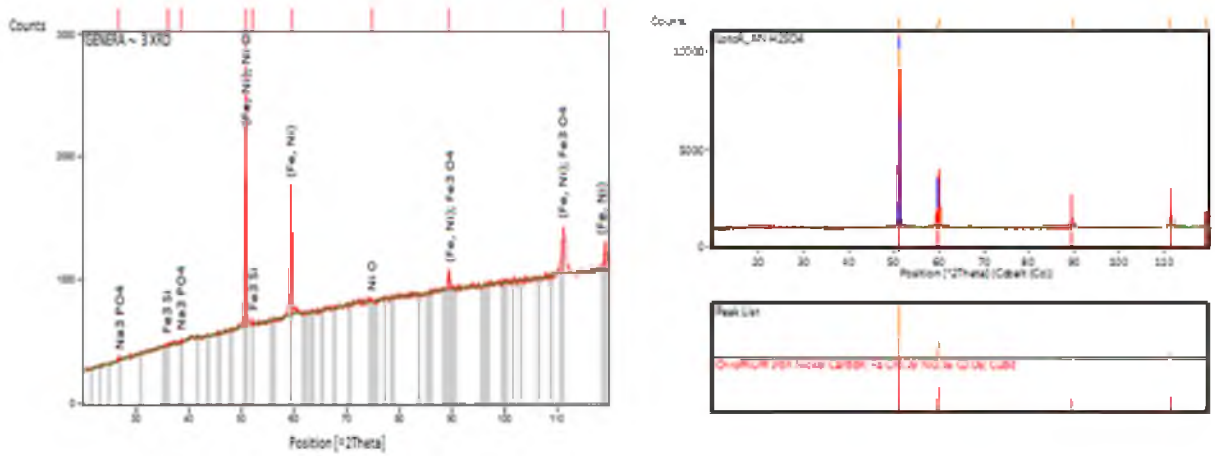

Figure 10: XRD pattern of the surface film formed (a) before immersion in the absence of AMB, (b) after immersion in the presence of AMB in 3 M H_2SO_4

Adsorption isotherm

Langmuir adsorption isotherm was applied to describe the adsorption mechanism for AMB compounds in 3 M H_2SO_4 solution, as it best fits the experimental results at 25 ^oC. The deviation of the slopes from unity in Fig. 11 is attributed to the molecular interaction among the adsorbed inhibitor species on the metal surface and changes in the values of Gibbs free energy of adsorption with increasing surface coverage. This was not taken into consideration during the derivation of the Langmuir equation. Langmuir isotherm predicts unity as the value of the slope. However, the fitted line gave a value less than unity for the slopes. This suggests a slight deviation from ideal conditions assumed in Langmuir model.

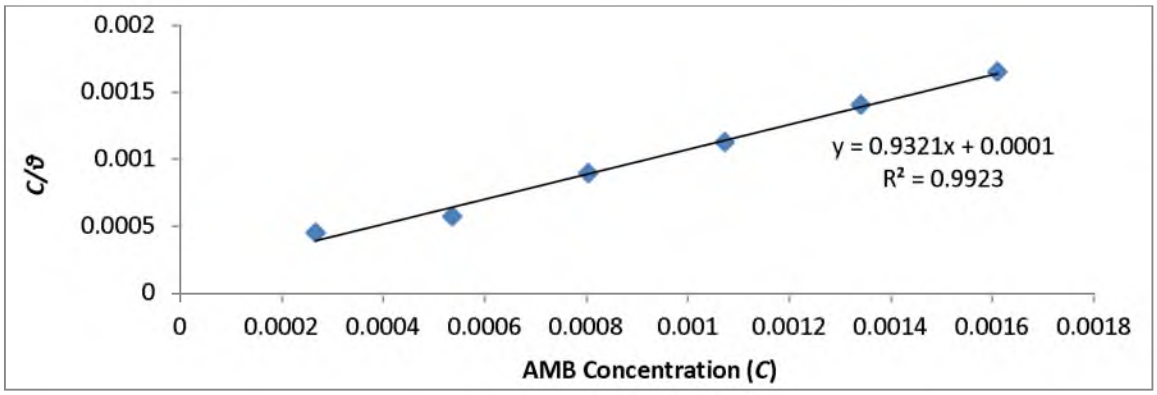

Figure 11: Relationship between $\frac{C}{\theta}$ and inhibitor concentration (C) in 3 M H_2SO_4

Copyrighted content, licensed for the sole use of:
Roland Loto, (3454331)

Thermodynamics of the corrosion process

The results presented in Table 5 provide additional evidence of slight deviation from ideal condition of Langmuir model as observed in the differential values of Free energy of Adsorption (ΔG_{ads}) with increase in surface coverage (θ) values. The dependence of free energy of adsorption (ΔG_{ads}) of AMB on surface coverage is ascribed to the inhomogeneous attributes of the stainless steel. On austenitic stainless steel not all sites can be equivalent on the surface due to heterogeneity, thus the differential adsorption energies as observed in the experimental data (Table 5). The value of ΔG_{ads} in H_2SO_4 and HCl reflects strong adsorption capability. The negative values of ΔG_{ads} showed that the adsorption of inhibitor molecules on the metal surface is spontaneous [33, 34]. The values of ΔG_{ads} calculated ranges between −31.33 and −35.43 kJ mol^{-1} for AMB in H_2SO_4.

Table 5 Data obtained for the values of Gibbs free energy, surface coverage and equilibrium constant of adsorption at varying concentrations of AMB in 3 M H_2SO_4

Inhibitor Concentration (*C*)	**Free energy of Adsorption (Δ*G*ads) (kJ/mol)**	**Surface Coverage (θ)**	**Equilibrium Constant of Adsorption (K_{ads})**
0.000268	-31.33	0.601	5620.4
0.000537	-35.43	0.940	29187
0.000805	-33.04	0.900	11134
0.001074	-34.41	0.954	19209
0.001342	-33.90	0.954	15520
0.001611	-35.03	0.976	25075

Statistical Analysis

The analysis in 3 M H_2SO_4 was evaluated for a confidence level of 95% i.e. a significance level of $\alpha = 0.05$. The ANOVA results in the acid solutions reveal only one of the experimental sources of variation (inhibitor concentration) to be statistically significant on the inhibition efficiency with F - values of 145.16 in H_2SO_4. These are greater than significance factor at $\alpha = 0.05$ (level of significance or probability). The F - values of exposure time in the solutions are less than the significant value factor hence they are statistically irrelevant. The statistical influence of the inhibitor concentration in H_2SO_4 (Fig. 13) is 95.75%. The influence of the exposure time is less than 0% thus practically negligible. The results using the ANOVA test is tabulated (table 6) as shown.

Copyrighted content, licensed for the sole use of:
Roland Loto, (3454331)

Table 6 Analysis of variance (ANOVA) for inhibition efficiency of AMB inhibitor in 3 M H_2SO_4 (at 95% confidence level)

AMB H_2SO_4					Min. MSR at 95% confidence	
Source of Variation	**Sum of Squares**	**Degree of Freedom**	**Mean Square**	**Mean Square Ratio**	**Significance F**	**F%**
Inhibitor concentration	7350.96	5	1470.19	145.16	2.71	95.75
Exposure Time	92.08	4	23.02	2.27	2.87	0
Residual	202.56	20	10.13			
Total	7645.60	29				

Conclusions

Phenylamine performed effectively as a corrosion inhibiting compound, reducing the corrosion rate of austenitic stainless steel at all concentrations studied from weight-loss, potential measurement and potentiodynamic polarization tests. The inhibition efficiency increased in direct proportion to increase in inhibitor concentration due to the availability of more inhibitor molecules to inhibit corrosion until saturation point. Adsorption of phenylamine on the stainless steel obeyed Langmuir's adsorption isotherm, producing the best fit, thereby indicating that the molecular interaction is fixed and the effect of lateral interaction among the adsorbates on the value of Gibbs free energy is negligible. XRD analysis of the steel specimen surface showed diffraction peaks for the inhibited steel surfaces revealing the absence of iron oxides and chemical compounds associated with corrosion. At a confidence level of 95% the ANOVA results in test solutions showed only the inhibitor concentrations to be statistically significant on the inhibition efficiency of aminobenzene.

References

1. Selvakumar P, Balanaga B K, and Thangavelu C, *Res J of Chem Sci* **3**(4) (2013) 87
2. Olsson C O A, Landolt D, *Electrochim Acta* **48** (2003) 1093
3. Bera S, Rangarajan S, and Narasimhan S V, *Corros Sci* **42** (2000) 1709
4. Taveira L V, Frank G, Strunk H P, and Dick L F P, *Corros Sci* **47** (2005) 757
5. Deflorian F, and Rossi S, *Electrochim Acta* **51** (2006) 1736
6. Mieczyslaw S, and Joanna T, *Int J Electrochem Sci,* **8** (2013) 9201
7. Negm N A, Mohamed A S, *J Surfactant Deterg* **7** (2004) 23.
8. Martin, R L, *ASM handbook*, ASM International, New York **13** (2003) 878.
9. Kane R D, *ASM handbook*, ASM International, New York **13** (2003) 922.

Copyrighted content, licensed for the sole use of:
Roland Loto, (3454331)

10. Negm N A, and Aiad I A J, *J Surfactant Deterg* **10** (2007) 87.
11. Bhaskaran R, Palaniswamy N, Rengaswamy, N S, and Jayachandran M, *ASM handbook*, ASM International, New York **13B** (2003) 621
12. Wojtanowicz A K, *Environmental technology in the oil industry*, Springer, Berlin **17** (2008) 51.
13. Trabanelli G, *Corrosion* **47** (1991) 410.
14. Ferreira E S, Giacomelli C F, Gicomelli F C, and Spinelli A, *Mater Chem Phys* **83** (2004) 129.
15. Bouklah M, Ouassini A, Hammouti B, and El Idrissi A, *Appl Surf Sci* **252** (2006) 2178.
16. Gopi D, Bhuvaneswaran N, Rajeswari S, and Ramadas K, *Anti-Corros Methods & Mater* **47** (2000) 332
17. Hosseini S M A, Salari M, and Ghasemi M, *Mater Corros* **60** (2009) 963.
18. Akrout H, Maximovitch S, Bousselmi L, Triki E, and Dalard F, *Mater Corros* **58** (2007) 202.
19. Gopi D, Manimozhi S K M, Govindaraju K M, Manisankar P, and Rajeswari S, *J Appl Electrochem* **37** (2007) 439
20. Popova A, Sokolova E, Raicheva S, and Christov M, *Corros Sci* **45** (2003) 33.
21. Noor E A, *Corros Sci* **47** (2005) 33.
22. Sk A, Ali M T, Saeed, and Rahman S U, *Corros Sci* **45** (2003) 253.
23. Chetouani A, Medjahed K, Sid-Lakhdar K E, Hammouti B, Benkaddour M, and Mansri A, *Corros Sci*, **46** (2004) 2421.
24. Dadgarnezhad A, Sheikhshoaie I, and Baghaei F, *Anti-Corros Method Mater* **51** (2004) 266.
25. Bouklah M, Ouassini A, Hammouti B, El Idrissi A, *Appl Surf Sci* **252** (2006) 2178.
26. Obot I B, Obi-Egbedi N O, and Odozi N W, *Corros Sci* **52** (2010) 923.
27. Satapathy A, Gunasekaran K G, Sahoo S C, Kumar A, Rodrigues P V, *Corros Sci* **51** (2009) 2848
28. Tao Z H, Zhang S T, Li W H, and Hou B R, *Corros Sci* **51** (2009) 2588.
29. Ferreira E S, Giacomelli C, Giacomelli F C, and Spinelli A, *Mater Chem Phys* **83** (2004) 129.
30. Cruz J, Martínez R, Genesca J, García-Ochoa E, *J Electroanal Chem*, 566(1) (2004)111.
31. Obot I B, Ebenso E E, Obi-Egbedi N O, Ayo S A, Zuhair M G, *Res Chem Intermed* **38**(2012) 1761
32. Quraishi M A, Rafiquee M Z A, Khan S, and Saxena N, *J Appl Electrochem* **37**(2007) 1153.
33. Obot I B, Obi-Egbedi N O, and Umoren S A, *Der Pharma Chemica* **1** (2009) 151.
34. Hosseini M G, Mertens S F L, and Arshadi M R, *Corros Sci* **45** (2003) 1473.

Copyrighted content, licensed for the sole use of:
Roland Loto, (3454331)